Optically Controlled Memristor Using Hybrid ZnO Nanorod/Polymer Material

Ayoub H. Jaafar

School of Physics and Astronomy, University of Nottingham, Nottingham, NG7 2RD, United Kingdom

Neil T. Kemp*

School of Physics and Astronomy, University of Nottingham, Nottingham, NG7 2RD, United Kingdom,
neil.kemp@nottingham.ac.uk

Controlling of resistive switching properties by optical means opens the route to new optoelectronics that can be written optically and read electronically. In this work, we demonstrate optically controlled memristors realized with a hybrid material of vertically aligned zinc oxide nanorods (ZnO NRs) and poly(methyl methacrylate) (PMMA). In addition to electronic switching, the devices are switchable by optical means upon illumination with UV light. The hybrid memristors require no forming step and exhibit multilevel switching behavior achieved by controlling either the DC sweep voltage or the UV light power. The optical memristor exhibits irreversible switching for the Off state, which has an important application in the fabrication of cloned neural networks with pre-trained information. The work provides a promising pathway for the fabrication of simple-to-make and low-cost optoelectronic devices for memory and optically tuned neuromorphic computing applications.

Keywords: optical memristor, bipolar switching, multilevel state, hybrid material

1 INTRODUCTION

Memristors have been attracting interest for nonvolatile memory technology due to their simple two-terminal Metal-Insulator-Metal (MIM) architecture, fast switching write/erase speeds, large on/off resistance window and low power consumption [1]. Memristors are also promising candidates for the development of high density and low power neural networks for brain-inspired artificial intelligent systems since they can mimic the neurobiological systems of the human brain [2]. Memristors are typically switched between two resistance states, i.e., from a high resistance state (HRS) to a low resistance state (LRS) and *vice versa* upon application of electric stimuli. Compared with electric stimuli, optical stimuli are more favorable to switch devices between the two resistance states owing to their high bandwidth communication, faster transmission speed, and noncontact input that can reduce the Joule heat effect on the devices [3,4]. In addition, varying the wavelength and intensity of optical stimuli enables dynamic control of learning and switching properties of

* Author to whom correspondence should be addressed.

memristors [4,5]. Developing optoelectronic memristor can also help to overcome the bottleneck limitations of traditional von Neumann computing architectures and the scaling down failing of Moore's law [6]. Optoelectronic memristors are also needed for future applications in artificial vision systems [7], photonic integrated circuits [8], and in-sensor reservoir computing systems [9].

To date, optoelectronic devices, namely, optical memristors, have been demonstrated in many materials including oxides [4,9–13], graphene oxide [14], low dimensional materials [15], and hybrid organic-inorganic materials [16]. Among them, hybrid organic-inorganic materials are promising candidates for fabrication optical memristors as they combine the electronic characteristics of semiconductors with the solution processing advantages of organic materials, such as low temperature processing, vacuum-free and large-area coverage at low costs on rigid and flexible substrates [17–19]. Hybrid materials, in comparison to organic- or inorganic-based memristors have shown excellent properties, such as reduced power consumption, ultra-low operation SET and RESET voltages, high on/off ratios, multi-level switching, analogue switching, and mechanical flexibility [17,20–23]. However, research studies on hybrid organic-inorganic materials based-optical memristors are very limited in comparison to the use of more conventional metal-oxide systems.

Here, we report for the first time an optical memristor based on a hybrid material consisting of ZnO NRs and PMMA polymer sandwiched between indium tin oxide (ITO) bottom and gold (Au) top electrodes. The device can respond to UV light with a wavelength of 405 nm. The optical memristor exhibits multistate storage that is achievable by controlling either the applied DC sweep voltage or the light power. Additionally, the devices show desirable characteristics including a forming-free bipolar resistive switching, low power consumption, and irreversible Off state after removal of the UV light.

2 EXPERIMENTAL

Vertically aligned ZnO NRs were grown in the same method reported earlier [24–26] using an ultrafast microwave heating process. Prior to the microwave growth step, a seed layer of ZnO nucleation sites was spin coated onto ITO bottom electrodes at 2000 rpm for 30 seconds using a 10 mM solution of zinc acetate dehydrate (98%, Aldrich) in propan-1-ol. Alignment of the nanorods was achieved by annealing the seeded layer on a hotplate at 350 °C for 30 minutes in air. The nanorod growth was achieved *via* submerging the samples upside down in a solution consisting of 25 mM zinc nitrate hexahydrate (Sigma Aldrich) and hexamethylenetetramine (HMTA) (Sigma Aldrich) in deionized water heated to a growth temperature of 80 °C. After 30 minutes of growth, the samples were removed, rinsed in DI water and dried by N_2. This was followed by deposition of the PMMA layer (Sigma Aldrich, dissolved in toluene) by spin-coating at 2000 rpm for 30 seconds. Afterwards, the samples were annealed on a hotplate at 140°C for 30 minutes to remove any unwanted solvent. The thickness of the PMMA layer was ~250 nm, measured by Dektak profilometry. Top Au (100 nm thick) electrodes were deposited by thermal evaporation under vacuum conditions through a shadow mask containing 400 μm diameter circles, giving a device structure of ITO/ZnO NRs/PMMA/Au. Note that control devices consisting of only ZnO NRs, ITO/ZnO NRs/Au, and only PMMA, ITO/PMMA/Au, were also fabricated. *I–V* characteristics and optical illumination were carried out using a Keithley 4200A-SCS Parameter Analyzer and an UV laser (Oxxius-405 nm), respectively.

3 RESULTS AND DISCUSSION

Figure1a schematically represents the hybrid organic-inorganic memristor. The optical properties of the ZnO NRs film were investigated using a UV-Visible absorption spectroscopy. The absorption spectrum is shown in Figure 1b. The absorption peak centered at 360 nm is the characteristic peak of pure ZnO [27,28]. Top view and tilted at 70° SEM images of ZnO NR arrays grown on ITO-coated glass substrate are shown in Figure 1c and 1d, respectively. The length and

diameters of ZnO NRs are about 200 nm and 40-60 nm, respectively. Note, the length of ZnO NRs appears to be longer due to the 70º sample tilt used in the SEM imaging. The figures show the hexagonal structure and very well packed and vertical alignment of ZnO NRs on the substrate, demonstrating the high-quality ZnO achieved *via* an ultrafast microwave growth technique.

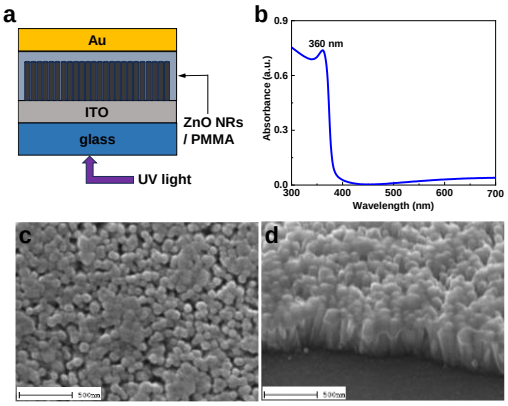

Figure 1: a) Schematic of the optical ZnO NRs/PMMA memristor. b) UV-Visible optical absorption spectrum of the ZnO NRs film grown on glass substrate. c) and d) Top view and tilted at 70° SEM images of the ZnO NRs, respectively.

The electrical properties of the memristors were characterized by DC voltage sweeps between the top and bottom electrodes. The devices were initially in HRS and showed a positive SET and negative RESET processes. Importantly, no forming process was needed to initiate the devices. We expect the lack of a forming step is because of the hydrothermal growth methods used to make the ZnO nanorods and nanoparticles, which both ensure a high concentration of defect states in the material. These pre-existing oxygen vacancies and non-lattice oxygen ions in ZnO bulk play a dominant role in forming-free resistive switching, as has previously been shown in ZnO based systems [24,29] as well as other systems containing appropriately added defects and/or migratory species [30].

Figure 2a shows a comparison study between three different device types. Two of the devices contain the ZnO NRs switching material, whereas the third device had only PMMA. The device containing only PMMA showed no resistive switching effect and had very low current over the sweep range of ±2.5 V, indicating highly insulating PMMA material. The device containing only ZnO showed bipolar resistive switching and had the highest currents reaching the compliance current (20 mA). Adding the PMMA layer to fabricate the hybrid device, decreased the On and Off currents and improved the switching characteristics. For instance, the On/Off ratio increased to 3 for the hybrid device compared with 1 and 1.5 for the PMMA- and ZnO-based devices, respectively. In addition, adding the PMMA layer to the ZnO decreased the power consumption from 1.3 mW for the ZnO device to 377 nW for the hybrid device, as shown in Figure 2b. The power consumption ($Power_{standby} = I_{HRS} \times V_{read}$) was calculated at a read voltage of 500 mV and the Off currents of the devices. Note, the hybrid devices showed compliance-free current behavior with a low operating switching voltage in comparison to previously reported literature on ZnO based-memristors [1,31]. These comparisons suggest the switching performance of inorganic ZnO can be improved by the incorporating of organic PMMA layer, making the hybrid devices promising candidates for fabrication low power consumption memristors.

The resistive switching in our hybrid memristor can be controlled upon changing the DC sweep voltages to achieve the multistate storage characteristics. Figure 2c illustrates the *I-V* curves of a device swept to different sweep voltages. The

plot clearly shows the device switches to different HRS levels upon varying the sweep voltage (±1.5 V, ±2.5 V and ±4 V), while the LRS remained the same. The effect is repeatable, as shown in Figure 2d. Thus, the device has four distinct multilevel resistance values including one LRS and three HRS. This multilevel effect is likely due to potentially larger electric field stress applied on the device upon increasing the voltage value [32,33].

The conduction mechanism of the ZnO and hybrid ZnO/PMMA devices is examined by plotting the positive part of the *I-V* curves for both devices in log-log scale. The fit for the ZnO device suggests that the conduction mechanism for both the HRS and LRS is governed by Ohmic conduction as the device exhibits a linear relationship between *I* and *V* ($I \propto V$), with a slope of ~1, as shown in Figure 3a. In contrast, the fit for the hybrid device indicates that the mechanism for the HRS and LRS is due to the Ohmic conduction at low applied voltage regions and space-charge-limit-current (SCLC) at high applied voltage regions, in which four conduction regions with different slopes can be identified, see Figure 3b. A similar conduction mechanism observed in our previously reported hybrid ZnO/PDR1A devices [26].

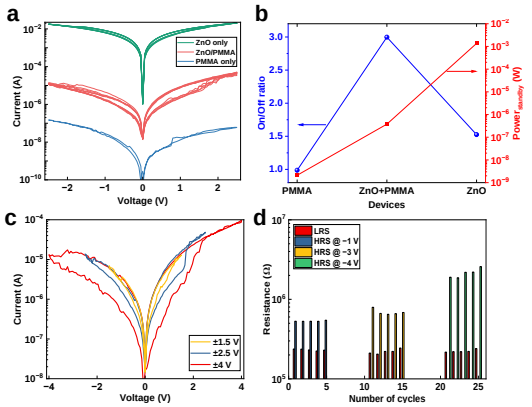

Figure 2: a) *I-V* characteristics of memristor devices based on ITO/ZnO NRs/Au (green curves), ITO/ZnO NRs/PMMA/Au (red curves), and ITO/PMMA/Au (blue curve). b) Current On/Off ratio and power consumption for different device types. c) *I-V* characteristics of a hybrid memristor at different sweep voltages. d) Multilevel states of the device with different sweep voltages. The resistance values of both HRS and LRS were read at 0.5 V.

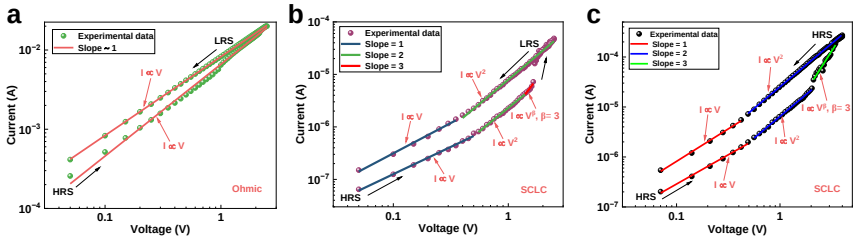

Figure 3: *I-V* characteristics in log-log scale for a) ITO/ZnO NRs/Au, and b) and c) ITO/ZnO NRs/PMMA/Au memristor under dark and UV conditions, respectively.

We will now demonstrate how the optical memristor can be controlled by light. Figure 4a and 4b show the *I-V* curves for ZnO and hybrid ZnO NRs/PMMA devices, respectively. The devices can switch between HRS and LRS in dark conditions (UV off). However, upon illumination with UV light at 405 nm (tuned to 20 mW), the electron-hole pairs can be generated, which switched both devices to higher current levels. Interestingly, the hybrid memristor showed a much

larger photocurrent response than the ZnO device. It is expected that adding the PMMA to the ZnO provides additional defect (trapping/releasing) sites at the ZnO/PMMA interface [34]. Under electric bias, these sites can trap charges to generate a sufficient internal field to switch the device between the two resistance states. However, illumination of the device with UV light excites electrons into the conduction band and causes more filling of traps at the interface, increasing the conductance of the device. After the UV light is switched off, the device showed a partial reversible switching effect, see green curve in Figure 4c. That is, to say, only the LRS current switched back into its initial level, while the HRS current did not. We ascribe this irreversible effect to partial release of holes trapped in the PMMA layer and/or at the interface since PMMA can inhibit the recombination process of charge carriers [35]. Note, it was found that the conduction mechanism for the hybrid optical device under UV light was also governed by SCLC, see Figure 3c. The effect of the UV on the operating mechanism is explained in detail in the last section below.

To further investigate the effect of light on the optical memristor, different UV light powers were used. It was found that the light switched the device from low current (UV off) to high current levels under different UV light powers, Figure 5a. The effect modulates not only the On and Off currents and the On/Off ratio, Figure 5b, but also modifies the HRS and LRS, resulting in multilevel resistance states, Figure 5c. Such a behavior suggests that the device has a potential application in high density multistate storage memory and neuromorphic computing systems [17,36].

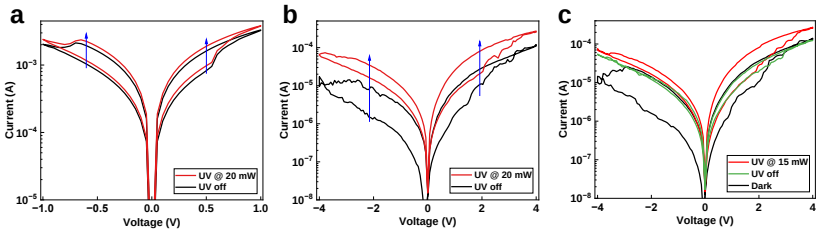

Figure 4: *I-V* curves under dark and UV illumination conditions for a) ZnO NRs device, b) hybrid ZnO NRs/PMMA device, and c) hybrid ZnO NRs/PMMA device under dark, UV illumination and after removal of UV light.

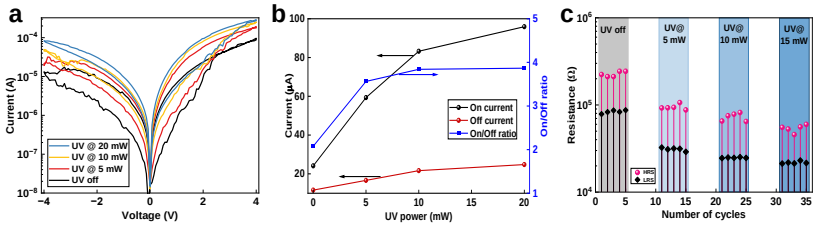

Figure 5: a) *I-V* curves of the optical memristor measured in dark and at different UV powers. b) On and Off current and the On/Off ratio as a function of UV powers. c) The HRS and LRS at different UV powers (extracted from *I-V* curves in Figure 5a at 2 V).

The operation mechanism for the hybrid optical memristor is suggested. The high concentration of defect states within the ZnO surface and at the ZnO/PMMA interface can serve as trapping sites and modify the internal dynamics of the charge carriers. As shown in Figure 3b and 3c, the *I-V* curves of the optical device in dark and under UV light fit the SCLC model. This suggests that the operating switching mechanism between SET and RESET processes is based on trapping and de-trapping effects upon application of an electric stimuli with different polarities. Such a process is consistent with the previously proposed operating mechanism for systems containing hybrid ZnO/PMMA materials [37,38]. Upon application of a positive voltage on the ITO electrode, electrons are initially injected from the Au electrode into the LUMO level of

PMMA *via* thermally generated carriers (Ohmic conduction, $I \propto V$). Increasing the voltage gradually increases the injection process *via* the SCLC, $I \propto V^2$, but the device remains in the Off state since the injected electrons are trapped by the defects at the ZnO/PMMA interface. Once the applied bias reaches the SET voltage and all the traps being fully occupied, $I \propto V^{\beta}$, the device switches from the Off state to the On state. However, reversing the voltage polarity releases the trapped charges, switching the device back into the Off state

Exposure of the hybrid optical memristor to the UV light significantly changes the electrical and switching properties of the device. The device exhibited a large photoconductance effect, which resulted in multilevel state switching. This effect is attributed to photogeneration of charge carries. Schematic diagrams of the band structure at the ZnO/PMMA interface under thermal equilibrium conditions are illustrated in Figure 6. The interface plays an important role in trapping and releasing the photogenerated charges for hybrid systems [39]. Illumination of the device, Figure 6a, excites electrons in the ZnO from the valence band into the conduction band, which results in the formation of photogenerated holes in the valence band [40]. The excited electrons cause a sizable increase in the conductance. Meanwhile, the photogenerated holes can move into the PMMA layer and be trapped by defects under the effect of applied electric stimuli. These trapped charges can also participate in increasing the conductance by reducing the effective barrier height at the interface. However, after removal the UV light, the device showed a reversible switching for the On state, but irreversible switching for the Off state. This suggests that some of the charges remain trapped in the PMMA layer, Figure 6b, and the electric stimuli cannot restore the device back to its initial state. The irreversible switching can be attributed to the introduction of PMMA layer, which can cause a prolongation of carrier lifetime decay at the interface for hybrid systems [35]. Such a behavior has an important application in setting the initial value of weights in neural networks to pre-defined values [14].

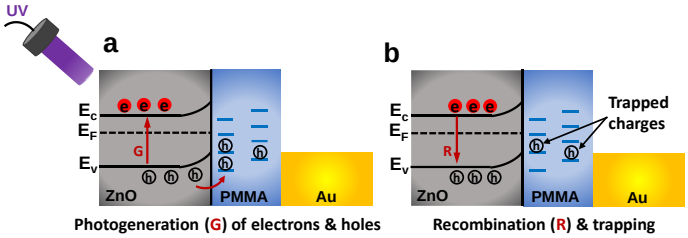

Figure 6: Schematic illustration the band diagram at the ZnO/PMMA interface, a) under UV illumination, and b) after removal the UV.

4 CONCLUSIONS

In this work, we have demonstrated an optical memristor based on a hybrid ZnO NRs/PMMA material. Besides electronic switching in dark conditions, the device can response to UV light at different powers, which enable the multilevel switching states. In addition, the hybrid memristor showed desirable characteristics including forming free operation, compliance-free bipolar nonvolatile switching, low-power operation, and long-term memory switching effects under UV stimulation. The results suggest an encouraging pathway toward fabrication of low cost and low power consumption optically tuned memristors for multistate storage memory and artificial intelligent applications.

ACKNOWLEDGMENTS

We would like to thank the Leverhulme Trust Research Project: RPG-2021-115 for partial support of this work. The authors would acknowledge the partial funding of this work from the Iraqi Ministry of Higher Education and Scientific Research.

REFERENCES

[1] J. Qi, M. Olmedo, J. Ren, N. Zhan, J. Zhao, J.G. Zheng, J. Liu, Resistive switching in single epitaxial ZnO nanoislands, ACS Nano, 6 (2012) 1051–1058.

[2] Y. Lee, C. Mahata, M. Kang, S. Kim, Short-term and long-term synaptic plasticity in Ag/HfO2/SiO2/Si stack by controlling conducting filament strength, Appl Surf Sci, 565 (2021).

[3] A.H. Jaafar, C. Lowe, A. Gee, N.T. Kemp, Optoelectronic Switching Memory Based on ZnO Nanoparticle/Polymer Nanocomposites, ACS Appl Polym Mater, 5 (2022) 2367–2373.

[4] Z. Zhou, Y. Pei, J. Zhao, G. Fu, X. Yan, Visible light responsive optoelectronic memristor device based on CeOx/ZnO structure for artificial vision system, Appl Phys Lett, 118 (2021).

[5] A.H. Jaafar, M.O. Neill, S.M. Kelly, E. Verrelli, N.T. Kemp, Percolation Threshold Enables Optical Resistive-Memory Switching and Light-Tuneable Synaptic Learning in Segregated Nanocomposites, Adv Electron Mater, 5 (2019) 1–7.

[6] A. Gee, A.H. Jaafar, N.T. Kemp, Optical Memristors: Review of Switching Mechanisms and New Computing Paradigms, in: Memristor Computing Systems, 2022: pp. 219–244.

[7] F. Zhou, Z. Zhou, J. Chen, T.H. Choy, J. Wang, N. Zhang, Z. Lin, S. Yu, J. Kang, H.S.P. Wong, Y. Chai, Optoelectronic resistive random access memory for neuromorphic vision sensors, Nat Nanotechnol, 14 (2019) 776–782.

[8] J.Y. Mao, L. Zhou, X. Zhu, Y. Zhou, S.T. Han, Photonic Memristor for Future Computing: A Perspective, Adv Opt Mater, 1900766 (2019) 1–15.

[9] Y. Sun, Q. Li, X. Zhu, C. Liao, Y. Wang, Z. Li, S. Liu, H. Xu, W. Wang, In-Sensor Reservoir Computing Based on Optoelectronic Synapse, Advanced Intelligent Systems, 5 (2023) 2200196.

[10] W. Zhou, R. Yang, H.K. He, H.M. Huang, J. Xiong, X. Guo, Optically modulated electric synapses realized with memristors based on ZnO nanorods, Appl Phys Lett, 113 (2018).

[11] P. Zheng, B. Sun, Y. Chen, H. Elshekh, T. Yu, S. Mao, S. Zhu, H. Wang, Y. Zhao, Z. Yu, Photo-induced negative differential resistance in a resistive switching memory device based on BiFeO3/ZnO heterojunctions, Appl Mater Today, 14 (2019) 21–28.

[12] C. Adda, H. Navarro, J. Kaur, M.H. Lee, C. Chen, M. Rozenberg, S.P. Ong, I.K. Schuller, An optoelectronic heterostructure for neuromorphic computing: CdS/V3O5, Appl Phys Lett, 121 (2022).

[13] L. Hu, J. Yang, J. Wang, P. Cheng, L.O. Chua, F. Zhuge, All-Optically Controlled Memristor for Optoelectronic Neuromorphic Computing, Adv Funct Mater, 31 (2021).

[14] A.H. Jaafar, N.T. Kemp, Wavelength dependent light tunable resistive switching graphene oxide nonvolatile memory devices, Carbon N Y, 153 (2019) 81–88.

[15] Y. Pei, L. Yan, Z. Wu, J. Lu, J. Zhao, J. Chen, Q. Liu, X. Yan, Artificial Visual Perception Nervous System Based on Low-Dimensional Material Photoelectric Memristors, ACS Nano, 15 (2021) 17319–17326.

[16] Y. Wang, Y. Xiong, H. Wang, X. Wu, J. Sha, Y. Shang, Y. Zhang, W. Li, S. Wang, Effect of P3HT passivation layer on triple cation organic-inorganic hybrid perovskite memristor, Current Applied Physics, 47 (2023) 54–59.

[17] A.H. Jaafar, L. Meng, T. Zhang, D. Guo, D. Newbrook, W. Zhang, G. Reid, C.H. (Kees) de Groot, P.N. Bartlett, R. Huang, Flexible Memristor Devices Using Hybrid Polymer/Electrodeposited GeSbTe Nanoscale Thin Films, ACS Appl Nano Mater, 5 (n.d.) 17711–17720.

[18] Ayoub H. Jaafar; Alex Gee; Abdullah O. Hamza; Charlotte J. Eling; Jean-Sebastien G. Bouillard; Ali M. Adawi; Neil T. Kemp, Evidence of Nanoparticle Migration in Polymeric Hybrid Memristor Devices, in: 2020 European Conference on Circuit Theory and Design (ECCTD), IEEE, 2020: pp. 1–4.

[19] A.H. Jaafar, A. Gee, N.T. Kemp, Printed and Flexible Organic and Inorganic Memristor Devices for Non-volatile Memory Applications, Journal of Physics D: Applied Physics - In Press, (2023).

[20] C. Gu, J.S. Lee, Flexible Hybrid Organic-Inorganic Perovskite Memory, ACS Nano, 10 (2016) 5413–5418.

[21] B. Hwang, J.S. Lee, Lead-free, air-stable hybrid organic-inorganic perovskite resistive switching memory with ultrafast switching and multilevel data storage, Nanoscale, 10 (2018) 8578–8584.

[22] J. Choi, S. Park, J. Lee, K. Hong, D.H. Kim, C.W. Moon, G. Do Park, J. Suh, J. Hwang, S.Y. Kim, H.S. Jung, N.G. Park, S. Han, K.T. Nam, H.W. Jang, Organolead Halide Perovskites for Low Operating Voltage Multilevel Resistive Switching, Advanced Materials, 28 (2016) 6562–6567.

[23] A.S. Sokolov, M. Ali, R. Riaz, Y. Abbas, M.J. Ko, C. Choi, Silver-Adapted Diffusive Memristor Based on Organic Nitrogen-Doped Graphene Oxide Quantum Dots (N-GOQDs) for Artificial Biosynapse Applications, Adv Funct Mater, 29 (2019).

[24] A.H. Jaafar, A. Gee, N.T. Kemp, Nanorods vs Nanoparticles: A Comparison Study of Au/ZnO-PMMA/Au Non-volatile Memory Devices showing the importance of Nanostructure Geometry on Conduction Mechanisms and Switching Properties, IEEE Transactions on Nanotehnology, 19 (2020) 236–246.

[25] R.J. Gray, A.H. Jaafar, E. Verrelli, N.T. Kemp, Method to reduce the formation of crystallites in ZnO nanorod thin-films grown via ultra-fast microwave heating, Thin Solid Films, 662 (2018) 116–122.

[26] A.H. Jaafar, R.J. Gray, E. Verrelli, M. O'Neill, S.M. Kelly, N.T. Kemp, Reversible optical switching memristors with tunable STDP synaptic plasticity: A route to hierarchical control in artificial intelligent systems, Nanoscale, 9 (2017) 17091–17098.

[27] J.H. Sun, S.Y. Dong, J.L. Feng, X.J. Yin, X.C. Zhao, Enhanced sunlight photocatalytic performance of Sn-doped ZnO for Methylene Blue degradation, J Mol Catal A Chem, 335 (2011) 145–150.

[28] M. Pudukudy, Z. Yaakob, Facile Synthesis of Quasi Spherical ZnO Nanoparticles with Excellent Photocatalytic Activity, J Clust Sci, 26 (2015) 1187–1201.

[29] Q. Mao, Z. Ji, J. Xi, Realization of forming-free ZnO-based resistive switching memory by controlling film thickness, J Phys D Appl Phys, 43 (2010).

[30] G. Milano, M. Luebben, Z. Ma, R. Dunin-Borkowski, L. Boarino, C.F. Pirri, R. Waser, C. Ricciardi, I. Valov, Self-limited single nanowire systems combining all-in-one memristive and neuromorphic functionalities, Nat Commun, 9 (2018).

[31] C. Chen, F. Pan, Z.S. Wang, J. Yang, F. Zeng, Bipolar resistive switching with self-rectifying effects in Al/ZnO/Si structure, J Appl Phys, 111 (2012) 1–7.

[32] A.H. Jaafar, L. Meng, Y.J. Noori, W. Zhang, Y. Han, R. Beanland, D.C. Smith, G. Reid, K. De Groot, R. Huang, P.N. Bartlett, Electrodeposition of GeSbTe-Based Resistive Switching Memory in Crossbar Arrays, Journal of Physical Chemistry C, 125 (2021) 26247–26255.

[33] S.Y. Wang, C.W. Huang, D.Y. Lee, T.Y. Tseng, T.C. Chang, Multilevel resistive switching in Ti/ Cux O/Pt memory devices, J Appl Phys, 108 (2010).

[34] M. Sulaman, Y. Song, S. Yang, S. Yang, M.I. Saleem, M. Li, C. Perumal Veeramalai, R. Zhi, Y. Jiang, Y. Cui, Q. Hao, B. Zou, Interlayer of PMMA Doped with Au Nanoparticles for High-Performance Tandem Photodetectors: A Solution to Suppress Dark Current and Maintain High Photocurrent, ACS Appl Mater Interfaces, 12 (2020) 26153–26160.

[35] J. Zeng, C. Meng, X. Li, Y. Wu, S. Liu, H. Zhou, H. Wang, H. Zeng, Interfacial-Tunneling-Effect-Enhanced CsPbBr3 Photodetectors Featuring High Detectivity and Stability, Adv Funct Mater, 29 (2019).

[36] D. Kumar, H. Li, U.K. Das, A.M. Syed, N. El-Atab, Flexible Solution-Processable Black-Phosphorus-Based Optoelectronic Memristive Synapses for Neuromorphic Computing and Artificial Visual Perception Applications, Advanced Materials, (2023).

[37] D. Son, D. Park, W.K. Choi, S. Cho, W. Kim, T.W. Kim, Carrier transport in flexible organic bistable devices of ZnO nanoparticles embedded in an insulating poly (methyl methacrylate) polymer layer, Nanotechnology, 20 (2009) 195203–195209.

[38] Z.L. Tseng, P.C. Kao, M.F. Shih, H.H. Huang, J.Y. Wang, S.Y. Chu, Electrical bistability in hybrid ZnO nanorod/polymethylmethacrylate heterostructures, Appl Phys Lett, 97 (2010) 95–98.

[39] X. Shan, C. Zhao, Y. Lin, J. Liu, X. Zhang, Y. Tao, C. Wang, X. Zhao, Z. Wang, H. Xu, Y. Liu, Optoelectronic synaptic device based on ZnO/HfOx heterojunction for high-performance neuromorphic vision system, Appl Phys Lett, 121 (2022).

[40] A. Manor, E.A. Katz, T. Tromholt, F.C. Krebs, Electrical and photo-induced degradation of ZnO layers in organic photovoltaics, Adv Energy Mater, 1 (2011) 836–843.